Bulletin of the Mineral Research and Exploration

http://bulletin.mta.gov.tr

Assessment of active tectonics based on GIS and statistical model: a case study of upper Alaknanda catchment (western Himalaya, India)

Adrija RAHA[a], Mery BISWAS[a] and Soumyajit MUKHERJEE[b*]

[a] *Department of Geography, Presidency University, 86/1, College Street, College Square, Kolkata 700 073, West Bengal, India*
[b] *Department of Earth Sciences, Indian Institute of Technology Bombay, Powai, Mumbai 400 076, Maharashtra, India*

Research Article

Keywords:
Geomorphic Indices, Index of Active Tectonics, Clustering, Himalayan Tectonics, Active Tectonics.

ABSTRACT

Due to continuing deformation of the Earth's crust, degradation and aggradation processes, the upper part of the Alaknanda basin lying in the Garhwal Himalaya, India, is considered to be tectonically active. Active tectonics in this region made a considerable impact on the drainage system and the topographic expression. Using a digital elevation model (DEM) with a resolution of 30 m * 30 m and based on eight geomorphic indices [hypsometric integral (HI), drainage texture (Dt), asymmetry factor (AF), ruggedness number (Rd), valley floor width/height ratio (Vfw), lemniscate coefficient (k) and basin shape index (Bs)], we evaluated active tectonics. Application of Index of Active Tectonic (IAT) and clustering model disclose the sub-watersheds in the southern part covering watersheds 16, 17 and near Badrinath sub-watershed 4, 9 and 8 are tectonically highly active (Class-1, 1.500-1.781). Cluster analysis defines two prominent clusters of sub-watersheds: 2, 4,14 and 15 in cluster 1; and 6, 7, 8 and 18 in cluster 2. Cluster 1 includes sub-watersheds 2, 4, 14, 15, and 16 and very high, high, and moderate IAT magnitudes. Sub-watersheds 6, 7, 8, and 18 are included in Cluster 2, which has very high and high tectonic activity.

Received Date: 29.08.2023
Accepted Date: 25.11.2024

1. Introduction

In the Himalayan landscape, tectonics is the most important factor forming the present-day topography, which could have an additional role of erosion/ denudation (Harkins et al., 2005; Andermann and Gloaguen, 2009; Perez-Pena et al., 2009). In the upper Alaknanda basin, crystallines of the Lesser and the Higher Himalaya exist at south and north, respectively (e.g., Metcalfe, 1993). This section of Alakanada catchment is composed of phyllites, slates and other metamorphic rocks (e.g., Celerier et al., 2009). It is possible to retrieve geomorphic evidence of active tectonics from topo-sheets, aerial photos, satellite information and through morpho-tectonic parameters (Horton 1945; Keller and Pinter, 2002). Morphometric investigation presents quantitatively the geometry of basins to comprehend initial slant or differences in the drainage basin's topography, geomorphic history, structural control, recent tectonics as well as rock hardness (Strahler, 1964). The Alaknanda River Basin is a tectonically active area with a history of destructive landslides and earthquakes. Landslides and/or seismicity has been reported frequently from locations such as Chamoli, Birahi, Pipalkoti and Rudraprayag. This area is traversed by several significant tectonically active thrusts e.g., the Main

Citation Info: Raha, A., Biswas, M., Mukherjee, S. 2025. Assessment of active tectonics based on GIS and statistical model: a case study of upper Alaknanda catchment (western Himalaya, India). Bulletin of the Mineral Research and Exploration 176, 1-16. https://doi.org/10.19111/bulletinofmre.1590821

**Corresponding author: Soumyajit MUKHERJEEB, soumyajitm@gmail.com, smukherjee@iitb.ac.in*

Central Thrust (MCT)- I, also known as the Vaikrita Thrust; MCT II, which is also known as the Munsiari Thrust; MCT III, also known as the Ramgarh Thrust, and the North Almora Thrust. (Shukla et al., 2014). Therefore morphological study in this area is an important exercise.

Even though several geomorphologic works have been undertaken on the Alaknanda river and the surroundings (review in Table 1), a morphometric study such as the preset work remained a due. This work involves hierarchical clustering of drainages and estimates Index of Active Tectonics (IAT) for different watersheds of the area taken into consideration. These are performed in order to understand the different degrees of tectonic activeness within the considered area.

Table 1- Geomorphic research done on Alaknanda river valley that partially or completely covers the study area of this work.

Sl no.	Reference	Aim	Key approach	Software used	Salient result
1	Bhattacharya and Jugran (1982)	To evaluate land subsidence as a landslide cause.	Ground truth has been used in conjunction with aerial photo interpretation.	-	The important factor in soil subsidence is seepage.
2	Barnard et al. (2001)	To comprehend the causes of landslides, both natural and anthropogenic.	Major landslides were mapped and samples from boulders on the surface were taken for cosmogenic radionuclide dating.	-	Human activity was responsible for ~ 2/3 of the landslides, primarily by removing toes of the slope at road cuttings.
3	Joshi and Kumar (2006)	To determine the relationship between historical occurrences of natural disasters and very heavy rainfall.	Daily rainfall data analysed statistically.	-	Frequent extreme rainfall is one of the main causes of landslides.
4	Sarkar et al. (2006)	To identify unstable slopes along the National Highway in the Alaknanda valley of Garhwal Himalaya.	Through photo documentation, probable slope failure zones were demarcated.	-	Mitigation of landslide-pone zones recommended.
5	Sati et al. (2007)	To attribute the development of the morphologic evidence along the North Almora Thrust.	Comprehending the Late Quaternary seismicity in the Alaknanda Valley near Srinagar from the morphologic evidence of Uttarak Fluvial terraces, entrenched stream channels, landslide-induced ponding, and active and stabilised landslide deposits.	-	NAT and its related lineaments are active in the Late Quaternary Period.
6	Sundriyal et al. (2007)	To carry out observations on lake deposits that have been impacted by landslides at the south-dipping, E-W and NW-SE trending North Almora Thrust.	Application of lithofacies, geochemistry and optically stimulated luminescence chronology.	-	Second and third order tributaries of the Alaknanda river were temporarily dammed due to activation of crumpled and unstable phyllite-dominated slopes. Seasonal deposition is indicated by sedimentary patterns of the succession under a transient lacustrine environment.
7	Kundalia et al. (2009)	To set rainfall thresholds for landslide initiation.	To determine the connection between rainfall amounts and the onset of a slope failure, an analytical approach is used.		Precipitation is the primary mechanism for slope failure.
8	Tyagi et al. (2009)	To locate areas of substantial surface uplift in the Alaknanda valley .	Application of steepness index.	ERDAS IMAGINE	Convex river profiles and high steepness index values identify areas that are experiencing quicker surface uplift. The zone of high uplift (incision) are the Main Central Thrust (MCT). South of the MCT, at Chamoli, Nand Prayag, and Karn Prayag.

Table 1- Continued.

9	Juyal et al. (2010)	To understand geographic and temporal variability in stages of aggradation/ incision in response to variations in climate and seismicity over the Late Quaternary in the Alaknanda valley.	Fill and strath terraces were mapped using total station survey. Paleoenvironmental reconstruction employed the fill sequences' sediment texture, structures and vertical lithostratigraphy. Infrared stimulated luminescence applied on feldspar grains.	-	Debris flow terraces formed during the early part of pluvial Marine Isotopic Stage 3 are the earliest fluvial landforms retained in the south of the Main Central Thrust.
10	Onagh et al. (2012)	To produce a landslide susceptibility map .	Multiple linear regression analysis using slope, aspect, lithology, land cover, rainfall, distances from fault, river, and road .	ILWIS 3.31 Academic, Arc GIS 9.3, Global Mapper 13.0 and Excel	The study area has been divided into Low, Moderate, High, and Very High relative landslip susceptibility classifications.
11	Parmar and Purohit (2013)	Mapping landslide hazard zones in Alaknanda Valley.	Lithology, structure, slope morphometry, relative relief, landuse and land cover, and hydrological conditions considered.		Shear zones, faults, heavily weathered and saturated sediments with unfavourable discontinuities characterize very high hazard zones.
12	Sarkar et al. (2013)	To evaluate the level of risk in the probable landslip zones, an effort has been made to quantify landslip intensity.	By assessing the severity of the present and possible landslides, landslip hazard assessment has been done to define the hazard levels. Individual landslides were initially subjected to hazard assessments in order to determine the possible risk of the research region.	ArcGIS *(version not referred)*	Most of the time, rock fall, rock slide and debris flow fall into the very high and high risk categories. To categorize the zones into different classes, the cumulative impact of landslide hazards was considered.
13	Shukla et al. (2014)	To assess the tectonic activeness using morphometric techniques and GIS .	Stream length ratio, bifurcation ratio, transverse topographic symmetry factor, asymmetry factor, drainage density, stream frequency, drainage texture form factor, circulatory ratio, and elongation ratio, valley width to valley height ratio, roughness number, the relief ratio, and the hypsometric integral have been computed on 8 sub basins.	Arc GIS 9.3, ERDAS 9.1 and MicroDEM software	The regions surrounding the MCT II (Munsiari Thrust), MCT III (Ramgarh Thrust), and North Almora Thrust, which are located in sub-basins 2, 3 and sections of 5 are tectonically quite active.
14	Chaturvedi et al. (2014)	Regional landslide susceptibility analysis using remote sensing.	A landslide susceptibility map was created involving lithology, fault, lineament, geomorphology, drainage, slope, aspect, land-use and land cover, soil texture, and soil depth.	-	After field validation, this method for susceptibility evaluation is fairly reliable and exact.
15	Devrani and Singh (2014)	To recognize the significance of location and regional elements in the valley filling process in an active mountain belt.	Hypsometry along with the lithofacies analysis were conducted .	ArcGIS 9.3	Sedimentation in the Pipalkoti valley stretch was mostly caused due to local reasons.
16	Gupta and Tandon (2014)	To identify the probable zones of instability, which causes frequent rock fall.	For each of the 23 locations where *in-situ* rocks are found, a kinematic rockfall hazard analysis was done.	-	The HH is mostly of low- to moderate-hazard, whereas the LH has a moderate- to high-hazard potential.
17	Chaudhary et al. (2015)	To understand the genesis of (paleo)valley.	The geomorphic configuration, sedimentological character, sediment source, flow velocity, and Optical Stimulated Luminescence (OSL) chronology have all been emphasised by authors.	ArcGIS 9.1	In the Alaknanda valley in the Central Himalaya, paleovalleys formed in two ways- (1) by significant valley aggradation, and (2) locally through landslides and lake breaching. Most of the Alaknanda valley's paleovalleys evolved between 15 to 8 ka, during significant valley aggradation.

Table 1- Continued.

18	Sajwan and Sushil (2016)	To examine the factors causing slope instability and landslides.	510 landslides identified in field. Landslides categorised as per rigidity and rockmass movements and debris that constitute the slided mass.		The atmospheric precipitation that causes landslides and flash floods can both be anticipated if real-time rainfall data is available.
19	Sundriyal et al. (2015)	To determine the type and reasons for the valley damage in June 2013.	Geochemical analysis of flood sediments.	-	Sediments came from two main sources: landslides from the Higher and Lesser Himalaya, and moraines and alluvial fans from the Trans and Higher Himalaya.
20	Chandak et al. (2016)	To highlight the locations at risk for landslides.	Information Value Method was adopted for landslide hazard mapping.	Integrated Land and Water Information System (ILWIS)	The unexpected dislodgment of small to large jointed blocks leads to rock avalanches / debris flows.
21	Rana et al. (2016 *a,b*)	To analyze the morphometric indices for neotectonic implications in a fluvial erosion-dominated regime.	Application of morphometric indices e.g., stream order, stream number, bifurcation ratio, drainage density, stream frequency, texture ratio, circularity ratio, basin hypsometry and elevation-relief ratio to assess neotectonic imprint upon the study area.	ArcGIS 9.3	The findings point to two high deformation/uplift zones in the valley: the first is in the Inner LH, close to the Main Central Thrust (MCT), and the second is in the Outer LH, south of the Tones Thrust.
22	Rana et al. (2016 *a,b*)	To categorize the seismic and aseismic categories for the fluvio-lacustrine sediment successions and valley-fill terraces.	Analyzing Soft sediment deformation structure and brittle deformation features in fluvial and fluvio-lacustrine deposits in the Alaknanda Valley.	-	Most of the deformation structures produced presumably in aseismic manner, although the terrain lies in the active seismic zone of the Central Himalaya.
23	Maurya et al. (2017)	To map probable landslide hazard zones in Badrinath, Garhwal Himalaya.	Application of GIS techniques .	ArcGIS 9.2	54% of the area has a high chance of landslides. Risk is moderate in 25% of the area.
24	Mehta et al. (2017)	To assess the change in terrain as an effect of 2013's disaster in Alaknanda and Mandakini basin.	The use of a field survey and a GIS technique allowed us to evaluate the changes in the topography.		Debris of 0.3 * 10^6 and 0.72 * 10^6 m^3 deposited at Govindghat and Pulna Village, respectively.
25	Prasad and Pandey (2017)	To evaluate the effects of LULC change, climate change, and their effects on hydrological hazard.	Both qualitative and quantitative methodologies. Peoples' perception about the origin of hazards, trend, frequency, magnitude, and mitigation measures were analyzed using a Likert-scale.		Households in the away district headquarter (ADH) village are more vulnerable than those in the near district headquarter (NDH) village. Due to their traditional and local knowledge of the responses to climate change, the NDH households had more potential for adjustment within the framing system.
26	Khanduri (2018)	To analyse and evaluate the effects of landslides in the Chamoli district.	Understanding the historical landslip episodes and resulting damages by overlying several thematic layers.	Arc View 9.3	These slides have been made possible in large part by the combination of heavy rainfall and the weak shear strength of the rocks.
27	Sharma et al. (2018)	To assess the relative active tectonics of the Alaknanda basin of Garhwal Himalaya.	Active tectonics in 8sub-basins of the Alaknanda basin using DEMs based on seismicity and 8 geomorphic indices.	ArcGIS 10.2	The middle portion of the tectonically most active sub-basin I exhibits movement rate of 41.1 mm y^{-1} in accordance with GNSS data.

Table 1- Continued.

28	Chauniyal (2018)	To locate the areas that have recently experienced uplift and displacement along the NAT in the Lesser Garhwal Himalaya's Lower Alaknanda Valley.	To identify places of neotectonic activity along N-S transverse faults.	-	Neotectonic movement along the NAT were noticeable between 15 to 9 ka and demonstrated recurring tectonics. Minor structures characteristic of Quaternary sediments identified.
29	Pant et al. (2020)	To identify the soil erosion and flood hazard zones using morphometric techniques.	Six primary morphotectonic parameters were examined on the upper Alaknanda basin and its sub-basins.	ArcGIS and SPSS (v.22)	Future development in the region should consider soil erosion, tectonic activity and potential for flash floods.
30	Khanduri and Rautela (2021)	To recognise the primary causes of slope instability.	In a GIS environment, the distribution of landslides has been connected with numerous parameters affecting their occurrence.	Arc Info 9.3	Landslides are most strongly influenced by proximity to the road and drainage system.
31	Meghanadh et al. (2021)	To generate a of landslide susceptibility map between Rudraprayag and Srinagar.	Multi-temporal interferometric synthetic aperture radar (MT-InSAR) and AHP approaches.	Sentinel Application Platform (SNAP) and Stanford Method of Persistent Scatterer (StaMPS)	There have been found 44.5% new landslide susceptible zones (LSZs).
32	Kumar et al. (2022)	To assess the vulnerable sites of slope instability along the NH-58 from Dhari Devi to Rudraprayag.	Kinematic analysis, geologic strength index, uniaxial compressive strength, rock quality designation, rock mass rating, slope mass rating and continuous slope mass rating are considered to assess slope instability.	-	Active landslides are caused by the Kaliasuar Fault in Uttarakhand. The Kaliasaur landslide is unstable due to pre-existing tectonic fracture and a plunging fold.
33	Joshi and Biswakarma (2023)	To compare models regarding landslide susceptibility mapping in the Alaknanda catchment area.	Application of Frequency Ratio Model, Analytic Hierarchical Process and Information Value Method to evaluate landslide susceptibility.	ArcGIS, Earth Resource Data Analysis System (ERDAS) IMAGINE	The Information Value Method yields the most precise results.
34	Clubb et al. (2023)	To evaluate sediment-storage mechanisms and identify the main influences on valley-floor morphology.	Application of the valley-floor width ratio throughout the Himalaya.	LSDTopoTools software	Long-term tectonically induced exhumation, not water discharge or bedrock erodibility, controls valley-floor width.
35	Raha et al. (this work)	To assess the active tectonics of the Upper Alaknanda Catchment.	Morphometric parameters such as Hypsometric integral (HI), Drainage texture (Dt), Asymmetry Factor (AF), Ruggedness number (Rd), Circularity Ratio (Rc), Valley Floor Width/Height Ratio (Vfw), Lemniscate Coefficient (k) and Basin Shape Index (Bs) are taken into consideration for the calculation of IAT. Cluster analysis has been performed on the sub-watersheds using dendrogram.	ArcGIS 10.3 and SPSS software (v26)	Tectonic activity is particularly high in the southern region where the NW-SE tectonic lineaments intersect with MCT II, encompassing sub-watersheds 16 and 17, and where numerous lineaments are present in various directions.

2. Geology

The upper catchment of the Alaknanda watershed lies under the Tethys Himalaya (TH) and is composed of Badrinath Granite and mostly the Central Crystallines. Towards south it is characterized by the Tethys Himalaya, the Higher Himalaya (HH), and a portion of the Lesser Himalaya (LH). Trans-Himadri Fault (THF) or the South Tibetan Detachment System (STDS) separates THS from HH. Main Central Thrust (MCT) is the boundary between the HH and the LH (Figure 1). The southern boundary of the LH is the Main Boundary Thrust (MBT). To the north and south of the Dudatoli syncline, respectively, the North Almora Thrust (NAT) and South Almora Thrust (SAT) divide the LH (Yin, 2006; Mukherjee, 2013). NAT is an out-of-sequence thrust and is presently active (review in Mukherjee, 2015).

With a variety of lithologies, dissection and drainage developments, the region is intricate. The litho-units in the study area are the Ramgarh Formation (lower crystalline zone) between the Munsiyari and Ramgarh Thrusts, the Munsiyari Formation (middle crystalline zone) between the Vaikrita and Munsiyari Thrusts, and the Vaikrita Group (upper crystalline portion lying between the STDS and the Vaikrita Thrust) (Srivastava and Mitra, 1994; Valdiya, 1995, 2001; Bhattacharya, 2008; Ray and Srivastava, 2010). In detail, the study area comprises of ten major geologic units- Badrinath Granite/ Tourmaline Granite, Baijanath Formation, Central Crystallines, Garhwal Group (Pithoragarh), Garhwal Group (Berinag), Martoli Formation, Rakcham Granite, Rawali Bagar Group, Sumna Group and an unamapped area (Figure 2).

3. Data acquisition and methods

From the Digital Elevation Model (DEM) of 30 m * 30 m spatial resolution of the SRTM the drainage lines were delineated. Based on the DEM (taken on 11-Feb-2000, released on 23-Sept-2014), watersheds were identified, evaluated and morphometric indices were generated (Table 2).

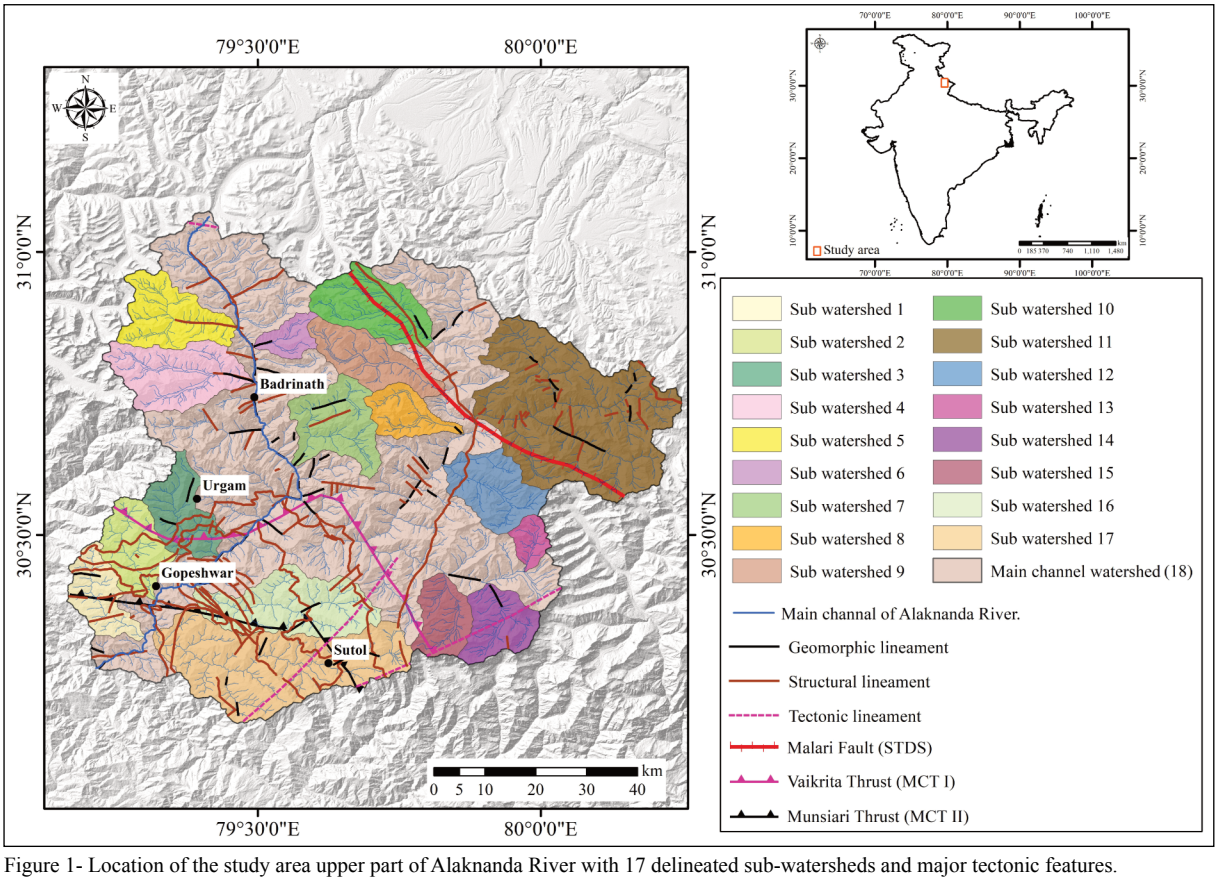

Figure 1- Location of the study area upper part of Alaknanda River with 17 delineated sub-watersheds and major tectonic features.

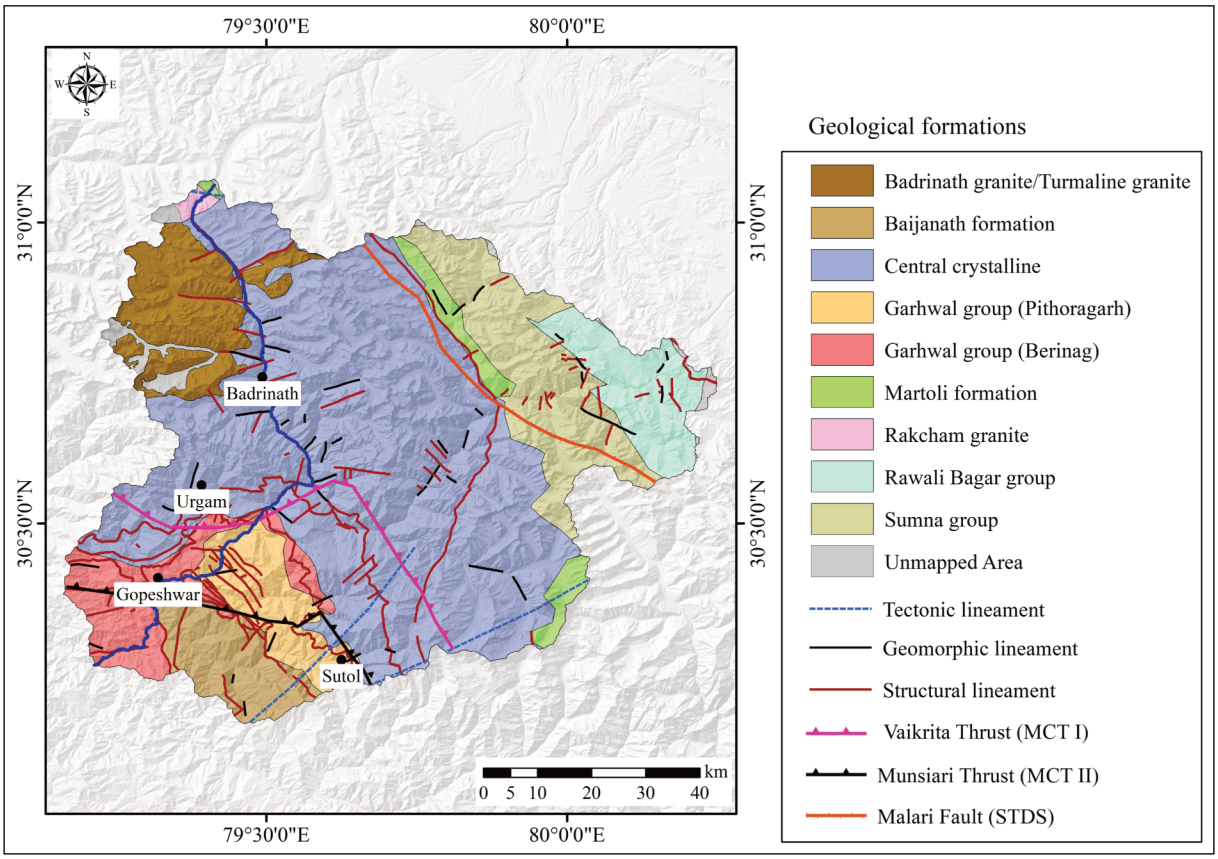

Figure 2- Map of general geology of the study area.

There were no clouds present when the photographs were taken. Therefore, no atmospheric correction was necessary. Several areal, linear and relief are assessed using the ArcGIS of the version of 10.3 (2014). The desired threshold value was utilized to create and extract the stream network using the D8 Python program incorporated in the ArcGIS itself. Slope directions have been deduced from each pixel to the eight-neighbour pixels. The watershed limits delineated by discrete flow angles and a single flow direction. The extracted drainage lines were mapped in the ArcGIS 10.3 (2014) platform. Seventeen sub-watersheds were delineated along the main channel of Alaknanda. The delineation of the sub-watersheds is based on the order of streams as per Strahler (1964). The streams of and above third order are considered for the delineation of the sub-watersheds. The lower order streams are not considered as the sub-watersheds do not have a considerable areal extent to understand the tectonic imprint upon them.

After careful review of the past literature, we have selected eight morphometric indices incorporating relief, areal aspects. The selected parameters are: Hypsometric integral (HI), Drainage texture (D_t), Asymmetry Factor (AF), Ruggedness number (R_d), Circularity Ratio (R_c), Valley Floor Width/Height Ratio (V_{fw}), Lemniscate Coefficient (k) and Basin Shape Index (B_s). The details of all the parameters along with its relevance in morpho-tectonic studies are listed in the Table 2. These are considered to calculate the IAT and to perform the clustering analysis using dendrogram for the considered watersheds. IAT ranks the watersheds as per their tectonic prioritization into four classes- very high, high, medium and low through mutual comparison. Magnitudes of these parameters have been grouped into four classes 1 to 4. The watersheds are categorized under low, moderate, high and very high classes in respect to tectonic activeness. The previously mentioned indices have been adopted for the selected seventeen sub watersheds as well as on the main channel watershed. The relation is:

Table 2- Details of equations and results of considered spatial and linear parameters for the study.

Sl. No.	Formula for basin scale indicators (unitlesss)	Equations & meaning of symbols	Explanations	References
1.	Hypsometric integral (HI)	$(\mathrm{Ele_{avg}} - \mathrm{Ele_{min}})$ $(\mathrm{Ele_{max}} - \mathrm{Ele_{min}})$ $\mathrm{Ele_{avg}}$: Average of elevation $\mathrm{Ele_{min}}$: Minimum elevation $\mathrm{Ele_{max}}$: Maximum elevation	The hypsometric integral is a dimensionless number that allows different sub-basins to be compared regardless of the scale. Hypsometric Integral indicates both tectonic activeness and lithological control. The rate of relief uplift is positively correlated with the hypsometric integral. HI value varies between 0 and 1 and a value nearer to 1 indicate a tectonically very active basin, 0.5 HI value is an indicator of equilibrium (mature) state and a value nearer to 0 indicates tectonically less active basin. Pike and Wilson (1971) mathematically derived the simpler form of hypsometric integral and shown proved that it is a valid approximation of actual hypsometric integral.	Strahler (1952) e.g. Chen et al. (2003); e.g. Pike and Wilson (1971); (Hamdouni et al., 2008).
2.	Elongation fatio (R_e)	$Re = 1.128\sqrt{\frac{A}{L_b}}$ A: signifies the area of the basin, Lb: denotes the length of the basin.	Elongation ratio is influenced by geology and climate. The values vary from 0 to 1 (e.g. Wołosiewicz, 2018). As the landscape evolves, the river basin becomes circular and the value tends to be 1.	Schumm (1956); e.g. Wołosiewicz (2018)
3.	Lemniscate coefficient (k)	$\mathrm{k} = \frac{\pi\, \mathrm{L_b^2}}{4\mathrm{A_B}}$ Where, A_B is the area of basin and L_b is the length of the basin.	Lemniscate coefficient based on expression at basin with Lemniscate curve (i.e. ratio of basin area to its length) in order to determine the shape of the basin. Higher Lemniscate values indicate an elongated basin, which in term denote tectonically very active drainage basin, whereas the low Lemniscate values are associated with less tectonically active basin.	Chorley (1957)
4.	Asymmetry factor (AF)	$AF = \left(\frac{A_r}{A_t}\right) * 100$ A_r: area of the basin (km^2) to the right of the main channel facing downstream and A_t: total area (km^2) of the basin.	An indicator to measure how much a river basin is tilted due to tectonics. Tectonic activity causes the main stream to change course, sloping away from the basin's midline.	Hare and Gardner (1985); e.g. Anand and Pradhan (2019)
5.	Ruggedness number (Hd)	$\mathrm{Hd} = \mathrm{R} * \mathrm{D}$ R = Basin relief D= Drainage density of the basin	Surface unevenness as topographic differentiation is measured.	Horton (1932)
6.	Valley floor width height ratio (V_{fw})	$V\mathrm{fwh} = \frac{2\mathrm{V_{fw}}}{[(\mathrm{E_{ld}} - \mathrm{E_{rd}}) + (\mathrm{E_{rd}} - \mathrm{E_{sc}})]}$ Here *Vf* w: width of the valley floor, E_{ld} and E_{rd}: elevations of the divide on the left and right side of the valley, respectively. *Esc*: average elevation of the valley.	This index differentiates between valleys with a wide floor relative to the height of valley dividers with a "U" shape compared to narrow, steep valleys with a "V" shape. Valleys with a U shape generally have high values of V_f, while V-shaped valleys with relatively low values. Since uplift is associated with incision, the index is thought to be a cause for dynamic tectonics where low values of V_f are associated with higher rates of uplift and incision. This index may be a degree of incision and not uplift; but in an equilibrium state, incision and uplift are nearly coordinated.	Bull and McFadden (1977)

Table 2- Continued.

7.	Drainage texture (D_t)	$D_t = Nu/P$ Nu: Number of streams of a given order. P: Perimeter (km) of the watershed.	The underlying lithology, infiltration potential, and relief characteristics of the terrain all affect drainage texture. Dt is the total number of stream segments in all orders along the watershed's edge (Horton, 1945). This is the relative channel spacing in fluidly prepared terrain, depending on many natural factors such as climate, precipitation, vegetation, rock / soil type, permeability, undulations, and watershed development stages. On the other hand, T is the product of Dd and F. It is calculated by multiplying the drainage density by the current frequency. If less than 4, T is classified as a coarse drainage texture. Intermediate drainage structure if it is between 4 and 10; fine drainage structure if it is between 10 and 15; ultrafine drainage structure if it exceeds 15 (Smith 1950).	Cox (1994)
8.	Basin shape index (Bs)	$Bs = \frac{Bl}{Bw}$ Bl: measured length from headwater to the point on the mouth of the basin, Bw: measured width at the widest point on the basin.	In the tectonically active area, the basin tends to be elongated.	E.g. Ramírez-Herrera (1998); Bull and McFadden (1977); Anand and Pradhan (2019)

$$IATc = \sum pn(1r + 2r + 3r \ldots . + nr)/N \quad \text{(equation 1)}$$

IATc: class of Index of Active Tectonics, p_n: parameter number, r: rank, N: number of parameters.

Clustering can discriminate signals (grouping signals) from noise (source signals). This technique works on unsupervised classification. Therefore, no prior assumptions are needed. This enables a better research outcome from the heterogeneous value ranges of the concerned indicators. In this study, hierarchical clustering is performed based on same indicators in sub-watershed scale. Using the Euclidean-based dissimilarity method, each segment was compared to its neighbours to assess how similar they were. The procedure was carried out using the following formula:

$$dR = (\sqrt{\sum_{i=0}^{n}(Xi - Yi)})/^{n} \quad \text{(equation 2; Clubb et al., 2014)}$$

Here n: number of segments, Xi: distance between the segments, Yi: difference in the steepness indices between the two profiles, i: component of the array, and dR: Euclidean-based dissimilarity. Using Ward's minimum variance method, hierarchical clustering was carried out using the dR values in the SPSS software (version 26, 2019). To show how each segment mutually relates, a dendrogram is created. Information about stress patterns is gathered from the World Stress Map (Internet reference 2: https://www.world-stress-map.org/ (Accessed on 16-Aug-2023).

4. Results

IAT was computed by taking the mean of the different classes of the areal and relief parameter. IAT values were sorted into four classes (Table 3) and mapped. As per the IAT analysis, sub-watersheds 4, 8, 9, 16 and 17 come under the tectonically very highly active region where IAT values under the range of 1.500-1.781. Sub-watersheds 6, 7, 10, 15 and 16 are under the magnitude of high tectonic activity (IAT = 1.782-2.063). The IAT range from 2.064-2.344 includes 1, 2, 3 and 14 sub watersheds, which are moderately active. Sub-watersheds at the NE portion as 11, 12 and 13 and at the NW part as 3 and 5 are under low range of active tectonic with IAT = 2.345-2.625 (Table 3). It is clear from the IAT map (Figure 3) that *(i)* tectonically active regions (watersheds 16 and 17) are characterized by the presence of Munsiyari Thrust (MCT II) that extends east-west. Besides there are NE-trending tectonic lineament and several multidirectional structural lineaments. *(ii)* Tectonically

Table 3- Class ranges and results of IAT analysis with magnitude.

Sub-watershed	Asymmetry Factor (AF)	Basin Shape (Bs)	Elongation Ratio(Re)	Lemniscate Coefficient (k)	Hypsometric Integral (HI)	Drainage Texture (Dt)	Ruggedness Number (Rd)	Valley Floor Width/ Height Ratio (Vfw)
1	6.955	1.836	0.709	1.989	0.383	1.963	21.462	0.030
2	4.619	2.029	0.683	2.143	0.426	2.135	29.896	0.016
3	1.666	2.089	0.656	2.323	0.465	1.795	47.841	0.164
4	8.518	2.046	0.672	2.214	0.469	4.621	52.415	0.070
5	1.324	1.248	0.819	1.488	0.509	3.476	32.595	0.420
6	13.396	1.422	0.679	2.167	0.474	1.760	18.309	0.576
7	19.142	1.096	0.780	1.643	0.511	4.146	49.232	0.125
8	18.105	1.618	0.629	2.522	0.524	3.401	45.456	0.098
9	0.695	2.645	0.549	3.319	0.460	2.361	58.393	0.209
10	16.025	1.856	0.729	1.878	0.398	3.996	53.190	0.402
11	4.388	1.219	0.923	1.172	0.461	5.704	24.294	0.173
12	0.127	1.434	0.790	1.601	0.523	4.443	31.643	0.230
13	6.122	1.432	0.697	2.057	0.426	1.454	36.302	0.704
14	8.260	1.436	0.806	1.537	0.367	2.641	58.522	0.026
15	10.702	1.937	0.745	1.799	0.513	2.741	54.558	0.272
16	4.579	2.216	0.604	2.740	0.367	2.342	46.025	0.044
17	2.736	2.348	0.608	2.701	0.313	5.037	45.065	0.023
Main channel watershed (18)	26.304	1.247	0.907	1.214	0.479	15.824	29.045	0.019

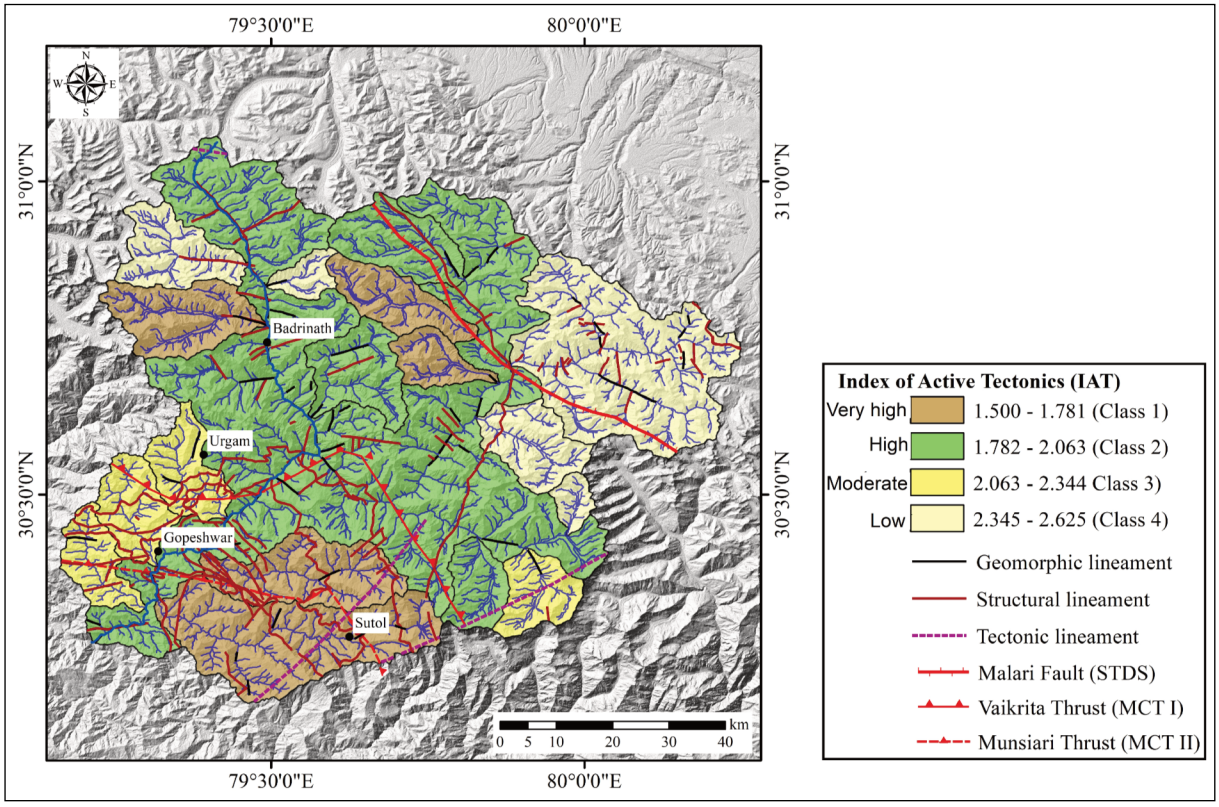

Figure 3- Map of Index of Active Tectonics (IAT) with 4 classes and 4 magnitudes as very high, high, moderate and low.

less active regions are distinguished by fewer presence or even absence of structural lineaments / faults.

The prepared dendrogram from the dR values enabled clustering of the calculated indicators of all watersheds (Figure 4). Cluster investigation of waterway profiles can compare the groups of similar waterway profiles inside heterogeneous scenes. The dR values are calculated to create a symmetric nearness lattice (Table 4). There are two major clusters as per the rescaled remove cluster combination. These are cluster 1 (sub-watersheds 2, 4 14, 15 and 16) and cluster 2 (sub-watersheds 6-8 and 18) (Table 4).

Table 4- Class ranges and results of IAT analysis with magnitude.

Class range	Magnitude	Sub-watersheds
1.500-1.781	Very High	4, 8,9, 16, 17
1.782-2.063	High	10,18,15
2.064-2.344	Moderate	1,2, 3, 14
2.35-2.625	Low	11,12,13

5. Discussions

Comparison between two methods as IAT and clustering done in this work indicate a positive similarity in assessing active tectonics of Alaknanda sub-watersheds. Cluster 1 covers watersheds 2, 4, 14, 15 and 16 belong to very high (1.500-1.781), high (1.782-2.063) and moderate (2.064-2.344) magnitudes of IAT. Cluster 2 covers sub-watersheds 6, 7, 8 and 18, which are under very high (IAT = 1.500-1.781) and high (IAT = 1.782-2.063) tectonic activeness (Table 5a,b).

Active thrust faults in the southern direction of the considered area covers sub watersheds 1, 2, 7, 16, and 18 (Figure 5). These watersheds belong to class 1 and 3 according to the IAT classes. Along the main channel of Alaknanda river near 20 km upstream of Gopeshwar, a hitherto unnamed strike-slip fault

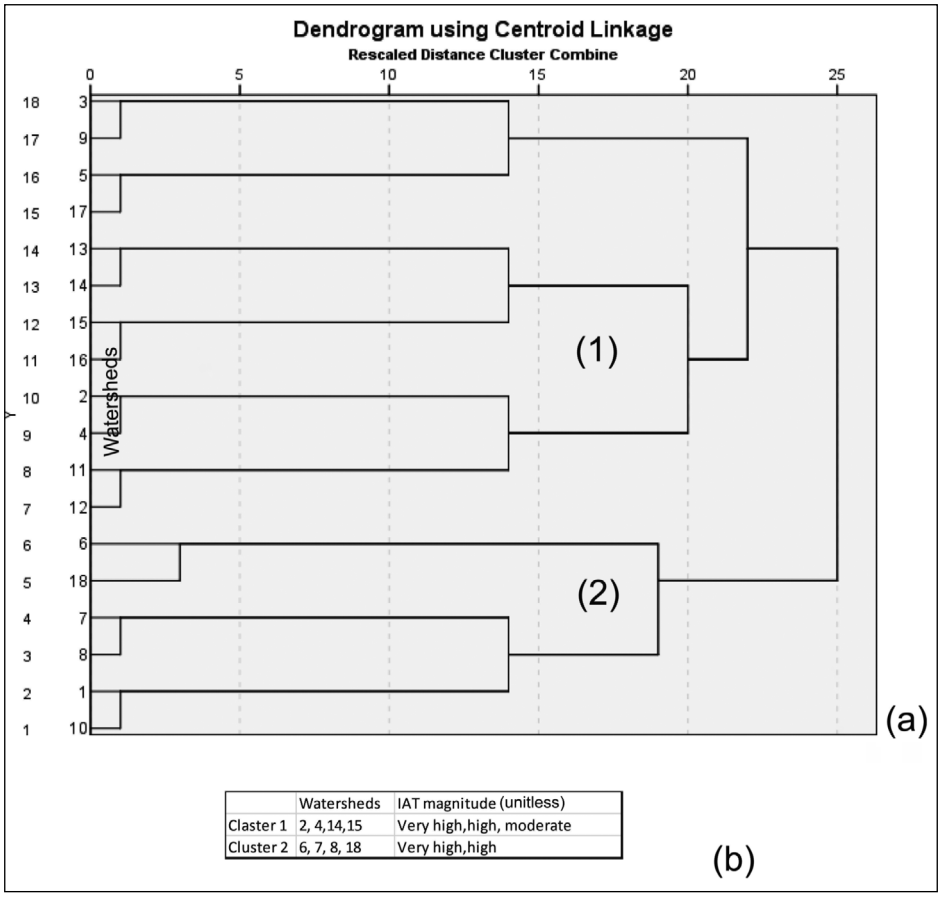

	Watersheds	IAT magnitude (unitless)
Claster 1	2, 4,14,15	Very high,high, moderate
Cluster 2	6, 7, 8, 18	Very high,high

Figure 4- a) Dendrogram showing two specific clusters, b) Considered watersheds under class 1 and 2.

Table 5a- Results of agglomeration schedule for calculating cluster 1 and 2.

Agglomeration Schedule						
Stage	Cluster Combined		Coefficients	Stage Cluster First Appears		Next Stage
	Cluster 1	Cluster 2		Cluster 1	Cluster 2	
1	5	12	3.358	0	0	6
2	16	17	11.599	0	0	4
3	4	15	13.126	0	0	7
4	3	16	14.503	0	2	13
5	7	8	16.956	0	0	10
6	2	5	17.929	0	1	9
7	4	14	25.790	3	0	11
8	1	11	29.720	0	0	12
9	2	13	34.458	6	0	14
10	7	10	36.056	5	0	15
11	4	9	60.159	7	0	13
12	1	6	71.818	8	0	14
13	3	4	97.740	4	11	15
14	1	2	129.028	12	9	16
15	3	7	149.008	13	10	17
16	1	18	262.847	14	0	17
17	1	3	468.580	16	15	0

Table 5b- Proximity Matrix (similarity) of 18 sub-watersheds.

Proximity Matrix																		
Case	Correlation between Vectors of Values																	
	1	2	3	4	5	6	7	8	9	10	11	12	13	14	15	16	17	18
1	1.000	0.986	0.960	0.987	0.957	0.929	0.994	0.995	0.954	0.998	0.972	0.943	0.987	0.985	0.992	0.976	0.964	0.813
2	0.986	1.000	0.993	0.999	0.991	0.854	0.967	0.966	0.991	0.986	0.984	0.983	0.999	0.999	0.997	0.999	0.994	0.725
3	0.960	0.993	1.000	0.991	0.998	0.792	0.934	0.933	1.000	0.962	0.974	0.994	0.991	0.993	0.986	0.998	0.997	0.650
4	0.987	0.999	0.991	1.000	0.991	0.862	0.973	0.971	0.987	0.989	0.990	0.983	0.998	0.999	0.998	0.997	0.993	0.747
5	0.957	0.991	0.998	0.991	1.000	0.786	0.933	0.930	0.998	0.961	0.984	0.998	0.987	0.991	0.983	0.996	0.999	0.670
6	0.929	0.854	0.792	0.862	0.786	1.000	0.955	0.958	0.777	0.926	0.843	0.756	0.866	0.856	0.882	0.829	0.799	0.914
7	0.994	0.967	0.934	0.973	0.933	0.955	1.000	1.000	0.925	0.996	0.960	0.915	0.973	0.969	0.981	0.954	0.939	0.855
8	0.995	0.966	0.933	0.971	0.930	0.958	1.000	1.000	0.924	0.995	0.956	0.911	0.972	0.968	0.980	0.953	0.937	0.851
9	0.954	0.991	1.000	0.987	0.998	0.777	0.925	0.924	1.000	0.955	0.971	0.995	0.987	0.990	0.981	0.996	0.997	0.635
10	0.998	0.986	0.962	0.989	0.961	0.926	0.996	0.995	0.955	1.000	0.976	0.946	0.989	0.987	0.994	0.977	0.966	0.815
11	0.972	0.984	0.974	0.990	0.984	0.843	0.960	0.956	0.971	0.976	1.000	0.982	0.980	0.984	0.982	0.981	0.987	0.784
12	0.943	0.983	0.994	0.983	0.998	0.756	0.915	0.911	0.995	0.946	0.982	1.000	0.977	0.982	0.972	0.989	0.997	0.652
13	0.987	0.999	0.991	0.998	0.987	0.866	0.973	0.972	0.987	0.989	0.980	0.977	1.000	0.999	0.999	0.997	0.989	0.728
14	0.985	0.999	0.993	0.999	0.991	0.856	0.969	0.968	0.990	0.987	0.984	0.982	0.999	1.000	0.999	0.998	0.992	0.726
15	0.992	0.997	0.986	0.998	0.983	0.882	0.981	0.980	0.981	0.994	0.982	0.972	0.999	0.999	1.000	0.994	0.986	0.755
16	0.976	0.999	0.998	0.997	0.996	0.829	0.954	0.953	0.996	0.977	0.981	0.989	0.997	0.998	0.994	1.000	0.997	0.693
17	0.964	0.994	0.997	0.993	0.999	0.799	0.939	0.937	0.997	0.966	0.987	0.997	0.989	0.992	0.986	0.997	1.000	0.685
18	0.813	0.725	0.650	0.747	0.670	0.914	0.855	0.851	0.635	0.815	0.784	0.652	0.728	0.726	0.755	0.693	0.685	1.000

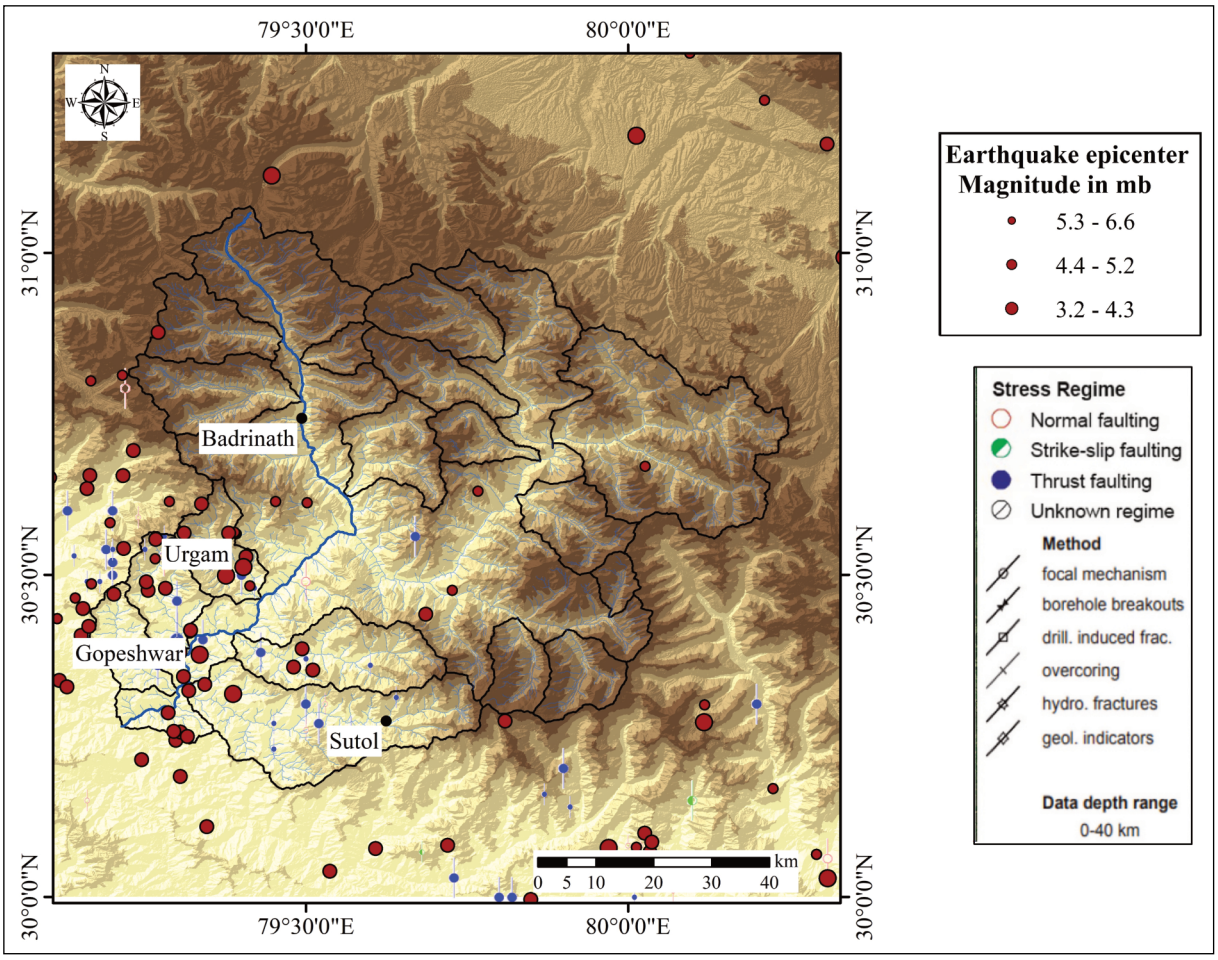

Figure 5- World stress map of the study area with 18 watersheds and IAT classes marked as C1-4.

exists (Figure 5). GPS time series data acquired near Gopeshwar disclose a high rate of displacement of 24.72 mm y^{-1} (Sharma et al., 2018). Major strike-slip and thrusts are located between the MCT I and MCT II (Figure 5).

Conclusions

For morphometric assessment of active tectonic, geomorphic indices that can be easily produced from the high resolution DEMs presently available through satellite observation are used. Such indices can be used to analyze data that covers a broader area quickly. We study 18 sub-watersheds of the upper Alaknanda basin in this work. Sub-watersheds 16 and 17 at the southern portion where NW-SE tectonic lineaments cross MCT II and where several lineaments exist in multi-direction, tectonic activity is very strong. High-to-moderate activeness was observed at the places on the periphery of the very high activity zone. This is also confirmed from cluster analysis.

Acknowledgements: Self-funded work. Thanks to the Chief Editor, Associate Editor, Reviewers, proofreaders and the publisher.

References

Andermann, C., Gloaguen, R. 2009. Estimation of erosion in tectonically active orogenies. Example from the Bhotekoshi catchment, Himalaya (Nepal). International Journal of Remote Sensing, 30(12), 3075-3096.

Anand, A., Pradhan, S. P. 2019. Assessment of active tectonics from geomorphic indices and morphometric parameters in part of Ganga basin. Journal of Mountain Science 16, 1943-1961.

Barnard, P. L., Owen, L. A., Sharma, M. C., Finkel, R. C. 2001. Natural and human-induced landsliding in the Garhwal Himalaya of northern India. Geomorphology 40, 21–35.

Bhattacharya, A., Jugran, D. K. 1982. landslide due to mass sinking phenomenon: Sunil-Joshimath of UP Himalaya example. Journal of the Indian Society of Photo-Interpretation and Remote Sensing, 10, 53-55.

Bull, W. B., McFadden, L. D. 1977. Tectonic Geomorphology North and South of the Garlock Fault, California. In: Doehring, D.O. (Ed) Geomorphology in Arid Regions: A Proceedings Volume of the 8th Annual Geomorphology Symposium, State University of New York, Binghamton, 115-138.

Celerier, J., Harrison, M. T., Webb, A. A. G. 2009. The Kumaun and Garwhal Lesser Himalaya, India: part 1. Structure and stratigraphy. Geological Society of America Bulletin, 121(9-10), 1262-1280.

Chandak, P. G., Sayyed, S. S., Kulkarni, Y. U., Devtale, M. K. 2016. Landslide hazard zonation mapping using information value method near Parphi village in Garhwal Himalaya. Ljemas 4, 228-236.

Chaudhary, S., Shukla, U. K., Sundriyal, Y., Srivastava, P., Jalal, P. 2015. Formation of paleovalleys in the Central Himalaya during valley aggradation. Quaternary International 371, 254–267.

Chauniyal, D. D. 2018. Evidences of Neo-Tectonic landforms between Srinagar and Bagwan area in Lower Alaknanda Valley (Garhwal Himalaya), India. In: Rosetti F et al. (Eds) CAJG 2018: The Structural Geology Contribution to the Africa-Eurasia Geology: Basement and Reservoir Structure, Ore Mineralisation and Tectonic Modelling. Springer, 323–326.

Chaturvedi, P., Dutt, V., Jaiswal, B., Tyagi, N., Sharma, S., Mishra, S. P., Dhar, S., Joglekar, P. N. 2014. Remote sensing based regional landslide risk assessment. International Journal of Emerging Trends Electrical Electronics 10, 135-140.

Chorley, R. J. 1957. Illustrating the laws of morphometry. Geological Magazine 94, 140-150.

Chen, Y., Sung, Q., Cheng, K. 2003. Along-strike variations of morphotectonic features in the Western Foothills of Taiwan: tectonic implications based on stream-gradient and hypsometric analysis. Geomorphology 56(1): 109-137.

Clubb, F., Mudd, S. M., Milodowski, D. T., Hurst, M. D., Slater, L. 2014. Objective extraction of channel heads from high-resolution topographic data. Water Resources Research 50, 4283–4304.

Clubb, F. J., Mudd, S. M., Schildgen, T. F., Van Der Beek, P. A., Devrani, R., Sinclair, H. D. 2023. Himalayan valley-floor widths controlled by tectonically driven exhumation. Nature Geoscience, 16(8), 739–746.

Cox, R.T. 1994. Analysis of drainage-basin symmetry as a rapid technique to identify areas of possible quaternary tilt-block tectonics: an example from the Mississippi Embayment. Geological Society of America Bulletin, 106(5), 571-581.

Devrani, R., Singh, V. 2014. Evolution of valley-fill terraces in the Alaknanda Valley, NW Himalaya: Its implication on river response studies. Geomorphology 227, 112–122.

Gupta, V., Tandon, R. S. 2014. Kinematic rockfall hazard assessment along a transportation corridor in the Upper Alaknanda valley, Garhwal Himalaya, India. Bulletin of Engineering Geology and the Environment 74, 315–326.

Hamdouni, R. E., Irigaray, C., Fern′andez, T., Chac′on, J, Keller, E. A. 2008. Assessment of relative active tectonics, southwest border of the Sierra Nevada (southern Spain). Geomorphology 96, 150–173.

Hare, P. W., Gardner, T. W. 1985. Geomorphic Indicators of Vertical Neotectonism along Converging Plate Margins, Nicoya Peninsula, Costa Rica. In: Morisawa M, and Hack JT, editors, Tectonic geomorphology. Proceedings of the 15th Annual Binghamton Geomorphology Symposium, Allen and Unwin, Boston. 123–134.

Horton, R. E. 1932. Drainage-basin characteristics. Transactions, American Geophysical Union. 13, 350-361.

Horton, R. E. 1945. Erosional development of streams and their drainage basins: hydrophysical approach to quantitative morphology. Geological Society of America Bulletin, 56, 275-370.

Harkins, N. W., Anastasio, David J., Pazzaglia, Frank J. 2005. Tectonic geomorphology of the Red Rock fault, insights into segmentation and landscape evolution of a developing range front normal fault. Journal of Structural Geology, 27(11), 1925-1939.

Joshi, V., Biswakarma, P. 2023. Bivariate statistical method and knowledge driven heuristic approach for the comparison of landslide susceptibility mapping in the Alaknanda Catchment area. Indian Journal of Geosciences, 77, 71-106.

Joshi, V., Kumar, K. 2006. Extreme rainfall events and associated natural hazards in Alaknanda valley, Indian Himalayan region. Journal of Mountain Science, 3, 228-236.

Juyal, N., Sundriyal, Y., Rana, N., Chaudhary, S., Singhvi, A. K. 2010. Late Quaternary fluvial aggradation and incision in the monsoon-dominated Alaknanda valley, Central Himalaya, Uttrakhand, India. Journal of Quaternary Science 25, 1293-1304.

Khanduri, S. 2018. Landslide Distribution and Damages during 2013 Deluge: A Case Study of Chamoli District, Uttarakhand. Journal of Geography and Natural Disasters, 8(2), 1-10.

Khanduri, S., Rautela, P. 2021. Key Landslide Triggers: A Case Study of Upper Alaknanda Valley, Uttarakhand Himalaya, India. International Journal of Earth Sciences Knowledge and Applications 3, 321-327.

Kumar, P., Thakur, M., Singh, T. N. 2022. Slope stability analysis of road cut slopes along NH-58 in Alaknanda Valley from Dhari Devi to Rudraprayag, Uttarakhand, India. Journal of Earth System Science 131, 82.

Kundalia, S., van Westen, C. J., Champatiray, P. K. 2009. Establishing precipitation thresholds for landslide initiation in the upper catchment of Alaknanda river, Uttarakhand, India. In Proceedings of the 2nd International Conference on Earth Observation for Global Changes–Chengdu, vol. 1417.

Maurya, A., Tripathi, S., Sinha, L. K. 2017. Landslide Hazard Zonation Map of Joshimath-Badrinath Region, India: Using Remote Sensing and GIS Technique. International Journal of Applied Research and Technology 2, 214-224.

Meghanadh, D., Tiwari, A., Dwivedi, R. 2021. Landslide susceptibility mapping using MT-InSAR and AHP enabled GIS-based multi-criteria decision analysis. Geomatics, Natural Hazards and Risk 12, 675–693.

Mehta, M., Shukla, T., Bhambri, R., Gupta, A. K., Dobhal, D. P. 2017. Terrain changes, caused by the 15–17 June 2013 heavy rainfall in the Garhwal Himalaya, India: A case study of Alaknanda and Mandakini basins. Geomorphology 284, 53–71.

Metcalfe, R. P. 1993. Pressure, temperature and time constraints on metamorphismacross the Main Central Thrust Zone and High Himalayan slab in the Garhwal Himalaya, Himalayan tectonics. Geological Society of India. Special Publication 74, 485–510.

Mukherjee, S. 2013. Channel flow extrusion model to constrain dynamic viscosity and Prandtl number of the Higher Himalayan Shear Zone. International Journal of Earth Sciences 102, 1811-1835.

Mukherjee, S. 2015. A review on out-of-sequence deformation in the Himalaya. In: Mukherjee S, Carosi R, van der Beek P, Mukherjee BK, Robinson D (Eds) Tectonics of the Himalaya. Geological Society, London. Special Publications 412, 67-109.

Onagh, M., Kumra, V. K., Rai, P. K. 2012. Landslide susceptibility mapping in a part of Uttarkashi district (India) by multiple linear regression method. International Journal of Geology, Earth and Environmental Sciences 2, 102-120.

Pant, N., Dubey, R. K., Bhatt, A., Rai, S. P., Semwal, P., Mishra, S. 2020. Soil erosion and flood hazard zonation using morphometric and morphotectonic parameters in Upper Alaknanda river basin. Natural Hazards, 103, 3263–3301.

Parmar, M. K., Purohit, K. 2013. Landslide Disasters in Uttarakhand: A Case of Landslide Susceptibility Zonation of Alaknanda Valley in Garhwal Himalaya. Global Journal of Current Research 2, 19-26.

Perez-Pena, J. V., Azanon, J. M., Azor, A., Delgado, J., Gonzalez, F. L. 2009. Spatial analysis of stream power using GIS: SLk anomaly maps. Earth Surface Process and Landforms 34, 16–25.

Pike, R. J., Wilson, S. E. 1971. Elevation-Relief Ratio, Hypsometric Integral and Geomorphic Area—Altitude Analysis. Geological Society America Bulletin 82, 1079-1084.

Prasad, A. S., Pandey, B. W. 2017. Climate change, Land use and land cover change direction and its impact on hydrological hazards and sustainabile development: A case study of Alaknanda river basin, Uttarakhand, India. Riscuri Si Catastrofe 20, 55-68.

Rana, N., Sati, S. P., Sundriyal, Y., Juyal, N. 2016*a*. Genesis and implication of soft-sediment deformation structures in high-energy fluvial deposits of the Alaknanda Valley, Garhwal Himalaya, India. Sedimentary Geology 344, 263–276.

Rana, N., Singh, S., Sundriyal, Y., Rawat, G., Juyal, N. 2016*b*. Interpreting the geomorphometric indices for neotectonic implications: An example of Alaknanda valley, Garhwal Himalaya, India. Journal of Earth System Sciences 125, 841–854.

Ray, Y., Srivastava, P. 2010. Widespread aggradation in the mountainous catchment of The Alaknanda–Ganga river system: timescales and implications to hinterland–foreland relationships. Quaternary Science Reviews 29, 2238–2260.

Ramírez-Herrera, M. T. 1998. Geomorphic assessment of active tectonics in the Acambay graben, Mexican Volcanic Belt. Earth Surf Process Landforms 23, 317–332.

Sajwan, K. S., Sushil, K. 2016. A geological appraisal of slope instability in Upper Alaknanda Valley, Uttarakhand Himalaya, India. Journal of Geology and Geophysics, 5, 1-7.

Sarkar, S., Kanungo, D. P., Patra, A. K. 2006. Landslides in the Alaknanda valley of Garhwal Himalaya, India. Quarterly Journal of Engineering Geology and Hydrogeology 39, 79–82.

Sarkar, S., Kanungo, D. P., Sharma, S. 2013. Landslide hazard assessment in the upper Alaknanda valley of Indian Himalayas. Geomatics. Natural Hazards and Risk 6, 308–325.

Sati, S. P., Sundriyal, Y. P., Rawat, G. S. 2007. Geomorphic indicators of neotectonic activity around Srinagar (Alaknanda basin), Uttarakhand. Current Science 92, 824-829.

Schumm, S. A. 1956. Evolution of Drainage Systems And Slopes In Badlands At Perth Amboy, New Jersey. Geological Society America Bulletin 67, 597-646.

Sharma, G., Ray, P. K. C., Mohanty, S. 2018. Morphotectonic analysis and GNSS observations for assessment of relative tectonic activity in Alaknanda basin of Garhwal Himalaya, India. Geomorphology 301, 108–120.

Shukla, D. P., Dubey, C. S., Ningreichon, A. S., Singh, R., Mishra, B. K., Singh, S. 2014. GIS-based morpho-tectonic studies of Alaknanda river basin: a precursor for hazard zonation. Natural Hazards 71, 1433–1452.

Smith, K. G. 1950. Standards for grading texture of erosional topography. American Journal of Science 248, 655–668.

Strahler, A. N. 1964. Quantitative geomorphology of the drainage basin and channel networks. In: Chow, V.T. (Ed.), Handbook of Applied Hydrology. McGraw-Hill Book Co, New York, 4–74.

Strahler, A. N. 1952. Hypsometric (area-altitude) analysis of erosional topography. Geological Society America Bulletin. 63, 1117–1142.

Srivastava, P., Mitra, G. 1994. Thrust geometries and deep structure of the outer and lesser Himalaya, Kumaon and Garhwal (India): implications for evolution of the Himalayan fold-and-thrust belt. Tectonophysics 13, 89–109.

Sundriyal, Y. P., Tripathi, J. K., Sati, S. P., Rawat, G. S., Srivastava, P. 2007. Landslide-dammed lakes in the Alaknanda Basin, Lesser Himalaya: Causes and implications. Current Science 93, 568-574.

Sundriyal, Y., Shukla, A. D., Rana, N., Jayangondaperumal, R., Srivastava, P., Chamyal, L. S., Sati, S. P., Juyal, N. 2015. Terrain response to the extreme rainfall event of June 2013: Evidence from the Alaknanda and Mandakini River Valleys, Garhwal Himalaya, India. Episodes, 38, 179–188.

Tyagi, A. K., Chaudhary, S., Rana, N., Sati, S. P., Juyal, N. 2009. Identifying areas of differential uplift using steepness index in the Alaknanda basin, Garhwal Himalaya, Uttarakhand. Current Science 1473-1477.

Valdiya, K. S. 1995. Proterozoic sedimentation and Pan-African geodynamic development in the Himalaya. Precambrian Research 74, 35–55

Valdiya, K. S. 2001. Reactivation of terrane-defining boundary thrusts in central sector of the Himalaya: implications. Current Science 81, 1418–1430.

Wołosiewicz, B. 2018. The influence of the deep-seated geological structures on the landscape morphology of the Dunajec River catchment area, Central Carpathians, Poland and Slovakia. Contemporary Trends in Geoscience 7, 1-11.

Yin, A. 2006. Cenozoic tectonic evolution of the Himalayan orogeny as constrained by along-strike variation of structural geometry, exhumation history, and foreland sedimentation. Earth-Science Reviews 76, 1–131.